Distinctive temporal profiles of detergent-soluble and -insoluble tau and Aβ species in human Alzheimer's disease

Koss, David J.; Dubini, Marina; Buchanan, Heather; Hull, Claire; Platt, Bettina

Published in:
Brain Research

DOI:
10.1016/j.brainres.2018.08.014

Publication date:
2018

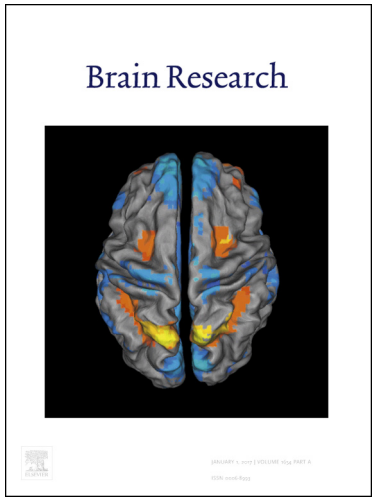

Research report

Distinctive temporal profiles of detergent-soluble and -insoluble tau and Aβ species in human Alzheimer's disease

David J. Koss, Marina Dubini, Heather Buchanan, Claire Hull, Bettina Platt

PII: S0006-8993(18)30434-7
DOI: https://doi.org/10.1016/j.brainres.2018.08.014
Reference: BRES 45911

To appear in: *Brain Research*

Received Date: 2 April 2018
Revised Date: 13 July 2018
Accepted Date: 9 August 2018

Please cite this article as: D.J. Koss, M. Dubini, H. Buchanan, C. Hull, B. Platt, Distinctive temporal profiles of detergent-soluble and -insoluble tau and Aβ species in human Alzheimer's disease, *Brain Research* (2018), doi: https://doi.org/10.1016/j.brainres.2018.08.014

Distinctive temporal profiles of detergent-soluble and -insoluble tau and Aβ species in human Alzheimer's disease

David J. Koss*, Marina Dubini, Heather Buchanan, Claire Hull, and Bettina Platt*

School of Medicine, Medical Sciences & Nutrition

College of Life Sciences and Medicine,

University of Aberdeen,

Aberdeen AB25 2ZD, UK

* Corresponding authors:
Dr David J Koss
University of Aberdeen
School of Medicine, Medical Sciences & Nutrition
Institute of Medical Sciences
Foresterhill
ABERDEEN AB25 2ZD
Scotland, UK
Email: d.koss@abdn.ac.uk

Current address:
Dr David J Koss
Newcastle University
Institute of Neuroscience
Campus for Aging and Vitality
Newcastle upon Tyne
NE4 6BE
England, UK
david.koss@ncl.ac.uk

Prof. Bettina Platt
University of Aberdeen
School of Medicine, Medical Sciences & Nutrition
Institute of Medical Sciences
Foresterhill
ABERDEEN AB25 2ZD
Scotland, UK
Tel.: (+44) 1224 437402
FAX: (+44) 1224 437465
Email: b.platt@abdn.ac.uk

Abstract

Alzheimer's disease (AD) pathology relevant proteins tau and beta-amyloid (Aβ) exist as an array of post-translationally modified and conformationally altered species with varying abundance, solubility and toxicity. Insoluble neurofibrillary tau tangles and Aβ plaques are end-stage AD hallmarks, yet may carry less disease significance compared to soluble species. At present, it is unclear how soluble and insoluble tau and Aβ relate to each other as well as to disease progression. Here, detergent soluble and insoluble fractions generated from post-mortem human temporal lobe samples (Brodmann area 21) were probed for tau and Aβ markers in immuno-dot assays. Measures were quantified according to diagnosis (AD cf. Non-AD), neuropathological severity, and correlated with disease progression (Braak stages). All markers were elevated within AD cases cf. non-AD controls ($p<0.05$) independent of solubility. However, when considered according to neuropathological severity, phospho-tau (detected via CP13 and AT-8 antibodies) was elevated early within the soluble fraction ($p<0.05$ intermediate cf. low severity) and emerged only later within the insoluble fraction ($p<0.05$ high cf. low severity). In contrast, PHF1 phospho-tau, TOC reactive tau oligomers and amyloid markers rose within the two fractions simultaneously. Independent of solubility, cognitive correlations were observed for tau makers and for fibrillary amyloid (OC). In contrast only soluble total Aβ was significantly correlated with intellectual impairment. Following the exclusion of end-stage cases, only soluble total Aβ remained correlated with cognition. The data indicate differential rates of protein aggregation during AD progression and confirm the disease relevance of early emerging soluble Aβ species.

Keywords

Alzheimer's disease, tau, β-amyloid, pathology, aggregation

1. Introduction

Senile (SP) and neuritic plaques (NP) composed of beta-amyloid (Aβ) together with intracellular tau-based neurofibrillary tangles (NFTs) constitute the neuropathological hallmarks of Alzheimer's disease (AD). The spatial quantification and characteristic spread of NFTs (Braak stages; Braak and Braak, 1995) and SP (Thal phases; Thal et al., 2002), alongside plaque density have been consolidated into a widely-adopted scheme for post-mortem neuropathological assessment (see the 'Consortium to Established a Registry for AD', (CERAD); Boluda et al., 2014).

Despite their utility in gauging AD related gross pathology, these hallmarks are not restricted to *bona fide* AD cases and can also emerge to a certain extent with age, often as subclinical neuropathology (see Spires-Jones et al., 2017, for review). For example, primary age related tauopathy (PART) cases present with modest AD-related Braak stage progression and mild cognitive impairment (MCI) in the absence of conventional Aβ pathology (Crary et al., 2014; Josephs et al., 2017). Similarly, post-mortem characterisation of non-demented individuals report a sub-population of cases in which substantial Aβ pathology is evident in the absence of significant cognitive impact, referred to as non-demented high pathological controls (HPC; Mufson et al., 2016) or pathologically diagnosed preclinical AD (p-PreAD; Upadhaya et al., 2014).

Such observations cast doubt on the causality of proteinaceous aggregates, particularly Aβ plaques, and their associations with cognitive impairment. Many post-mortem studies have reported a robust increase in SP and NP in AD cases, but indicate modest to no significant correlation between plaque load and cognitive deficits (Arriagada et al., 1992; Näslund et al., 2000; Giannakopoulos et al., 2003) or disease duration (Ingelsson et al., 2004). In comparison, greater agreement exists between NFT pathology and mental decline (Giannakopoulos et al., 2003; Markesbery et al., 2006).

Nevertheless, given the well-established stereotypical emergence of NFTs (Braak and Braak, 1995) as well as SP (Thal et al., 2002) and their invariable presence within AD pathology, such lesions are unlikely to be inconsequential. Conceptually, plaques and tangles may sequester more toxic yet less aggregated species into tightly bound, insoluble fibrils. This deposition may diminish their toxic potential and ubiquity, and reduce widespread neuronal damage whilst generating a secondary localised insult. It is equally plausible that specific subpopulations of deposited aggregations may retain a toxic potential whilst others are rendered inert (Ladiwala et al., 2010+ 2011; Cowan et al., 2015). Indeed, animal models have demonstrated that the presence of NFTs within neurons is neither conducive to physiological failure (Kuchibhotla et al., 2014) nor to cognitive impairment (Santacruz et al., 2005).

Naturally, post-mortem histopathological determination of protein aggregates relies on end stage pathologies and utilises broad measures of quantification which may fail to account for the heterogeneity of insoluble and soluble structures. This limits our causal

understanding of pathological processes and the modifications driving Aβ and tau to adopt mature aggregated depositions.

Both Aβ and tau share common schemes of aggregation, as monomers form prefibrillar oligomers followed by fibrillary intermediates or oligomers, which are incorporated into protofilaments prior to maturation in filamentous SPs and NFT aggregates (reviewed in Serpell, 2000; Kuret et al., 2005; Ruggeri et al., 2015). The aggregation process is closely linked to the adoption of β-sheet conformations, which results in decreased solubility in aqueous solutions, with higher order assemblies soluble only in solvents such as Hexafluoroisopropanol (HFIP) and formic acid (Burdick et al., 1992; Halverson et al., 1990). The generation of conformation-specific antibodies raised against tau (MC-1 (Jicha et al., 1997); TOC1 (Patterson et al., 2011) and Aβ (A11 and OC, Kayed et al., 2007) in various states of aggregation have helped to validate multiple intermediate Aβ and tau species as immune-reactivity distinct. Specifically, TOC1 recognises an exposed epitope within tau which is natively accessible only upon oligomerisation (Ward et al., 2014). Accordingly, a number of studies have shown early stage elevations in TOC1 reactivity within tauopathy mouse models (Ward et al., 2014) and human tissue (Patterson et al., 2011 and Koss et al., 2016). The amyloid-selective OC antibody recognises a common and conserved conformation within all fibril amyloid proteins, independent of amino acid sequence (Kayed et al., 2007). In relation to Aβ, the OC epitope is rapidly formed from isolated soluble monomers and present within low weight fibrillar oligomers prior to formation of more mature Thioflavin T positive fibrils, themselves also OC reactive (Coalier et al., 2013).

Across the spectrum of tau and Aβ assemblies a profile of graded toxicity is emerging. Soluble prefibrillar oligomers are suggested as most toxic (Walsh and Selkoe, 2007, Lasagna-Reeves et al., 2011; Castillo-Carranza et al.; 2014; Cox et al., 2016) and strongly index cognitive decline (Koss et al., 2016). However, both soluble and insoluble fibrillary oligomers are also reported to exert a significant level of toxicity (Ladiwala et al., 2010). In addition, non-toxic soluble and insoluble, so-called off-pathway aggregates have also been reported (Cowan et al., 2015, Ladiwala et al., 2010 +2011; Sharoar et al., 2012; Bieschke et al., 2011).

In biological tissues the isolation of Aβ and tau configurations are commonly achieved via multistep fractionation exploiting their variable degree of solubility. Monomeric and low weight prefibrillary species can be extracted within aqueous buffers with or without mild non-ionic detergents, whilst larger aggregates can be solubilised in strong denaturing agents such as formic acid or isolated by their insolubility in a 1% sarkosyl solution (see Rostagno and Ghiso et al., 2009; Julien et al., 2012 for review).

Prior work suggests that even within middle-aged non-AD cases as much as 30-45% of total Aβ can be isolated from a detergent insoluble fraction by formic acid, the percentage rising to 97-99% in AD brains (Wang et al., 1999). The overlap of gross insoluble Aβ levels between AD and control cases has led to a weak predictive value for AD diagnosis (Näslund et al., 2000; Tremblay et al., 2007). Despite soluble Aβ levels representing only 1-2% of total Aβ

within the AD brain a more robust correlation with disease severity has been reported (McLean et al., 1999, Wang et al., 1999; Koss et al., 2016).

In contrast to Aβ, the vast majority of tau protein can be isolated within aqueous or detergent soluble fractions. In non-AD cases, as much as 97% of tau can be recovered from the soluble fraction, whilst in AD this is considerable lower (~50%) due to the accumulation of insoluble aggregates (Mukaetova-Ladinska et al., 1993; Tremblay et al., 2007; Han et al., 2017). Insoluble tau isolated from human AD brains is 3-4-fold higher compared to non-AD brains (Hanger et al., 1991; Ksiezak-Reding et al., 1992) and levels within temporal and parietal regions are robustly elevated mirroring the regional burden of NFTs. This acts as a good indicator of disease progression, correlating with Braak staging as well as CERAD scores and various cognitive measures (Mukaetova-Ladinska et al., 1993; Tremblay et al., 2007). Nevertheless, soluble tau species also demonstrate increased phosphorylation at many of the same sites observed in insoluble AD tau (Matsuo et al., 1994, Zhou et al., 2006 and Koss et al., 2016). Investigations into presumed toxic tau species have identified a number of immunological distinct conformations (Jicha et al., 1997) as well as prefibrillar and fibrillary aggregation states (Patterson et al., 2011; Lasagna-Reeves et al., 2012) in addition to phospho-tau species. However, it remains unclear how soluble tau species relate to the hyperphosphorylated, insoluble aggregates.

Despite the growing number of identified molecular entities comprising tau and Aβ pathology and their abundance in human AD brains, few studies have sought to determine the emergence of such species within the context of one another. Following on from our previous characterisation of soluble AD pathology within the temporal lobe of human AD cases we here present further data assessing both soluble and insoluble tau and Aβ species in relation to AD diagnosis, neuropathological severity and cognitive decline. Moreover, we sought to evaluate OC reactive amyloids as a potentially improved or additional measure of pathology.

2. Results

2.1 Detection of distinct soluble and insoluble immunoreactive species

To preserve the native conformations of extracted soluble species and to avoid size based exclusion issues during SDS/PAGE, dot-blots were used for the detailed quantification of soluble cf. insoluble tau and Aβ species. Prior to this, the extraction of distinct tau and Aβ configurations within the two fractions was confirmed via Western blotting (Fig. 1). Tau species isolated within the soluble fraction when resolved on SDS page migrated as defined protein bands compared to smears obtained from the insoluble fraction. This was particular apparent for the pan-tau antibody HT-7 (Fig. 1A,) as well as phospho-tau antibody CP13 (Fig. 1B), although some smearing was evident upon applying enhanced contrast (see Suppl. Fig. 1). Interestingly, the distinction between soluble and insoluble tau species was not as evident with PHF1 reactive tau species, which migrated across a broad range of molecular weights (25->220kDa) independent of fraction (Fig. 1C).

Soluble Aβ detected with MOAB-2 was evident across the length of the gel (Fig. 1D). Despite only weak immunoreactivity for monomeric Aβ (~4 kDa, see Suppl. Fig. 1D for enhanced contrast), more intense reactivity was concentrated around the 35-60 kDa region and within material retained within the loading wells. The range of immunoreactivity within the soluble fraction differed from the predominate detection of 40 to 220 kDa migrating MOAB-2 reactive material in the insoluble fraction. Western blot analysis of Aβ with pan Aβ antibody 6E10 robustly detected a 4 kDa reactive band corresponding to the monomeric peptide in both soluble and insoluble fractions (see Suppl. Fig. 2).

Under SDS page conditions only limited OC reactive species were detected in both the soluble and insoluble fraction. It is notable that due to the conformational nature of the antibody, only those aggregates which are not denatured upon SDS exposure would remain in a detectable configuration (Coalier et al., 2013). Nevertheless, an increased OC signal (two bands evident at 40-60 kDa) was seen in AD cases when compared to non-AD controls within the soluble fraction as well as in the mid-range smears from the insoluble fraction (Fig. 1E).

For most blots (insoluble fraction for all antibodies and soluble PHF1 fraction) little to no immunoreactivity was evident in non-AD cases for optimised exposure settings. Following contrast enhancement of blots where signals from AD cases were saturated, weak signals emerged in non-AD samples in most cases (see Suppl. Fig. 1).

Immunoreactivity in both soluble and insoluble fractions for all antibodies were subsequently quantified in dot blots with ECL signals being normalised to total protein as established via a Coomassie membrane stain (see Suppl. Fig. 3 for example Coomassie stained membrane images).

2.2 Tau

Total tau dot blot signals from isolated soluble and insoluble fractions demonstrated a 3 and 4 fold increase in immunoreactivity, respectively, in accordance with AD diagnosis ($p<0.0001$, for both Fig. 2 i+ii). Increased HT-7 reactivity in both fractions was evident between high neuropathology cases compared to those classed as low neuropathological cases ($p<0.001$, Fig. 2 iii), yet only in the soluble fraction was an increase between intermediate and high pathology cases observed ($p<0.001$, Fig. 2 iii).

Correlations of HT-7 immunoreactivity with individual Braak staging reported an increased correlative strength for soluble tau compared to the insoluble fraction ($r=0.72$; $p<0.01$ compared to $r=0.57$; $p<0.01$ for soluble and insoluble measures, respectively, Fig. 2 iv). For both severity and individual Braak stage classification, high levels of variability may have prevented detection of a significant increase relative to pathology free cases (Br0) within the insoluble fraction, HT-7 immunoreactivity differed reliably only between Br6 and Br0 cases ($p<0.05$). Levels of soluble and insoluble tau were modestly related within individual cases (Spearman's correlation, $r=0.48$, $p<0.0001$). Further statistical tests via a 2-way ANOVA with Braak stage and fraction as factors reported a significant effect only of Braak stage ($p = 0.0001$). As floor level effects at Braak stage 0 and ceiling level effects at Braak stage 5-6 may influence these statistical interrogations, a further 2-way ANOVA was run including only data from Braak stages 2-4. These stages represent the phase of progressive neuropathology within the temporal lobes and hence the point of conversion from non-AD and AD. However, again only a significant effect of Braak stage ($p<0.01$) was reported. Full details and associated F values for 2-way ANOVA are given in Suppl. Table 1.

2.3 Phospho-tau

The phospho-tau antibody AT8 is universally employed for immunohistological Braak staging. Both soluble and insoluble tau pathology can be detected via AT8 in the form of pre-tangle pathology and NFT containing neurons, respectively. Accordingly, comparative dot blots demonstrated increased AT8 reactivity in both fractions ($p<0.0001$ for both, Fig. 3A i+ii).

AT-8 immunoreactivity was consistently detected in all cases within the soluble fraction independent of diagnosis, and only one non-AD case was without discernible immunoreactivity in the corresponding insoluble fraction.

In line with the assumption that soluble pre-tangle neurons represent the precursors of mature NFTs, elevations from low neuropathology cases in AT8 reactive tau were more readily apparent from the soluble (low cf. intermediate, $p<0.01$ and low cf. high, $p<0.001$; Fig. 3A iii) than in the insoluble fraction (low cf. intermediate, $p>0.05$, low cf. high, $p<0.001$). This differentiation was particularly apparent for Braak 4 (Braak stage 4 vs Braak stage 0 cases: $p<0.05$, Fig. 3A iv), preceding the later stage rise in insoluble AT8 reactive tau (Br6,

p<0.05). Both fractions reported a high level of correlation across Braak staging, (r=0.81, p<0.01) cf. insoluble AT8 data (r=0.75, p<0.01) as well as between each other (r=0.62, p<0.0001).

As observed for AT8, CP13 reactive insoluble tau was detected in the majority of samples (93% of non-AD cases and 100% of AD cases). Insoluble CP13 reactivity was elevated in a diagnosis specific manner (p<0.01; Fig. 3B i+ii), yet only significantly raised in the high (p<0.001; Fig. 3B iii) but not intermediate neuropathological cases relative to low pathology cases (p>0.05). This late stage elevation was in contrast to soluble CP13 tau which demonstrated increased immunoreactivity across all severity groups (low cf. intermediate p<0.01, low cf. high p<0.001, Fig. 3B iii) and may suggest CP13 as having greater sensitivity for earlier soluble phospho-Tau species (Koss et al., 2016).

In line with correlations observed for AT8, measurements of CP13 phospho-tau aligned with progressive Braak stages (r=0.78 and r=0.65, for soluble and insoluble respectively, p<0.01 for both; Fig. 3B iv). CP13 reactivity between fractions from each case also strongly correlated (r=0.68, p<0.0001). High variability prevented any individual Braak stage from reaching significance relative to Braak stage 0 for data from the insoluble fraction, in constrat to soluble fraction with was already elevated by Braak stage 2.

In contrast to the profile of CP13 and AT8, insoluble PHF1 reactive tau demonstrated a significant elevation not only dependent on AD diagnosis (p<0.0001; Fig. 3C i+ii) but also between intermediate and low pathology cases as well as between high and low pathological cases (p<0.001; Fig. 3C iii). Equally, the correlation of progressive phosphorylation at the PHF1 epitope with Braak stage was comparable for both soluble and insoluble measurements (r=0.83; p<0.01; Fig. 3C iv), strongly correlated with each other (r=0.82, p<0.0001), and reached significance from Braak 0 cases at Braak stage 4 and 5, respectively (p<0.05, for both). Although PHF1 immunoreactivity reported increased sensitivity for intermediate stage pathology as well as the greatest correlation with Braak staging, when considered alongside AT8 and CP13, a number of samples for both non-AD (7 out of 20, 35%) and AD (2 out 18, 11.11%) were without detectable reactivity for PHF1 in the insoluble fraction.

All phospho-specific antibodies reported a significant effect of Braak stage (p<0.01) following a 2-way ANOVA across all Braak stages. However, only PHF-1 yielded both an interaction (p<0.05) as well as a significant effect of fraction (p<0.001), presumably due to the magnitude of change between soluble and insoluble preparations. Bonferroni post-tests indicated that the significance of fraction was largely driven by Braak stage 6 (p<0.001). Focusing on the progressive phase of pathology (Braak stage 2-4), all phospho-tau antibodies reported significant effects of Braak stage (p<0.001) as well as fraction (p<0.05) and an interaction for CP13 and AT8 (p<0.0001). Post-tests revealed that differences at Braak stage 4 drove the significance of fraction (p<0.0001) for both CP13 and AT8. Full details are given in Suppl. Table 1.

Given that post-mortem interval (PMI) may alter protein phosphorylation, i.e. proteins may become dephosphorylated following death, all phospho-tau values were investigated for a significant relationship with PMI duration. No significant correlation was observed between any phospho-tau marker or indeed any other marker examined and hours prior to post-mortem, for either soluble or insoluble fractions.

2.4 Oligomeric Tau

TOC1 immunoreactivity was detected in both soluble and insoluble fractions. Although this antibody preferentially binds to prefibrillar conformations, assumed to be largely soluble in aqueous solutions, end labelling of more mature insoluble tau fibrils has also been observed (Patterson et al., 2011; Ward et al., 2014).

Insoluble reactivity was significantly raised in AD cases ($p<0.05$, Fig. 4 i+ii), and elevated in late stage high pathological cases compared to those with low neuropathology ($p<0.001$ Fig. 4 iii). These findings are largely in line with observations from the soluble fraction (as previously reported Koss et al., 2016). When correlated with Braak stage, soluble and insoluble TOC1 measures were of comparable strength ($r=0.61$ cf. 0.60, respectively, $p<0.01$, Fig. 4 iv). Again, as for PHF1 a strong correlative agreement was observed between soluble and insoluble levels of TOC1 ($r=0.78$, $p<0.0001$). However, insoluble TOC1 reactive material reported a significant elevation from Braak 0 cases only at the last pathological stage (Br 6; $p<0.05$). A 2-way ANOVA across either all Braak stages or Braak stage 2-4 reported only a significant effect of Braak stage ($p<0.01$, see Suppl. Table 1).

2.5 Aβ

Quantification of monomeric Aβ using 6E10 failed to detect significant differences between groups according to diagnosis or severity classifications within the insoluble lysates, despite elevations in the soluble fraction (see Suppl. Fig. 2 i-iii. In light of the previously reported technical considerations related to quantification of Aβ via Western blotting with the 6E10 antibody (Koss et al. 2016), we here quantified total Aβ using the MOAB-2 antibody which does not cross-react with APP or non-Aβ metabolites (Youmans et al., 2012). Quantification via dot blot reported robust immunoreactivity in all cases, independent of fraction (Fig. 5 i). Quantification of total Aβ within the insoluble fraction was significantly elevated across AD diagnosis ($p<0.05$, Fig. 5 ii), yet only an overall trend within severity classifications ($p=0.075$, Fig. 5 iii) was observed no correlation across individual Braak stages was reported ($p>0.05$). When compared within individual cases a modest agreement between soluble and insoluble levels was reported ($r=0.49$, $p<0.001$). The large degree of overlap between diagnosis groups as well as within severity classifications quantified in the insoluble fraction is in contrast to the improved separation of signal strength seen in the soluble fraction, particularly between diagnosis groups (as previously reported Koss et al., 2016, non-AD cf.

AD, $p<0.0001$, overall severity effect, $p<0.0001$ and correlation with Braak stage, $r=0.7$, $p<0.001$). Potentially influenced by the high variability of signal obtained in the insoluble fraction, neither Braak stage ($p>0.05$) or fraction ($p>0.05$) were reported as significant variables in 2-way ANOVA, both when considered across the entire Braak staging scale and when limited to progressive pathological stages for the temporal lobe (Braak stages 2-4). See Suppl. Table 1 for details.

2.6 Fibrillary amyloid

We next investigated the amino acid sequence independent fibrillary amyloid antibody, previously shown to react with toxic fibrils comprised of amyloids (Ladiwala et al., 2011). Accordingly, OC immunoreactivity in both soluble and insoluble sample fractions was dependent on diagnosis (Fig. 6 i+ii; $p<0.0001$ for both), as well as neuropathology severity (Fig. 6 iii; overall $p<0.001$, for both). Significance across severity classifications was principally driven by the increased signal detected in high severity cases compared to those with low levels of pathology ($p<0.001$ for both), although specifically in the soluble fractionation, a further distinction between intermediate and high neuropathology was also reported ($p<0.05$). Equally, correlation of OC immunoreactivity with Braak staging was greater for the soluble fraction (Fig. 6 iv; $r=0.68$, $p<0.01$; insoluble: $r=0.58$, $p<0.01$). However, a robust relationship between soluble and insoluble quantification was evident ($r=0.64$, $p<0.0001$) and regardless of solubility, a prominent increase in the levels of OC reactive material was apparent in cases determined as Braak stage 4 cf. Braak stage 0 ($p<0.05$). Subsequent tests utilising 2-way ANOVA reported Braak stage as the only significant variable ($p<0.001$) when considered either across all Braak stages or when limited to Braak stages 2-4 (See Suppl. Table 1).

2.7 Inter-marker correlations (Tau and Amyloid)

In line with the beta-amyloid cascade hypothesis, it can be speculated that an accurate measurement of Aβ pathology, either from within a soluble or insoluble fraction, should correlate to a degree with the level of tau pathology within a particular brain region. Whilst itself not evidence for causality, such a relationship would serve to support the validity of the hypothesis.

Strikingly, correlations between tau and amyloid markers revealed a robust pattern such that only soluble Aβ as established by MOAB-2 reported a degree of correlation with each of the markers of tau pathology from both fractions (Table 1). In contrast, measures of insoluble MOAB-2 reactivity failed to correlate significantly with the any tau measures. OC-immunoreactivity established from the soluble fraction demonstrated comparative correlations with tau pathology in relation to those observed with soluble MOAB-2 signals. Furthermore, moderate correlations were reported for insoluble OC measures and the majority of tau markers.

2.8 Pathological marker association with disease progression and cognitive decline

The majority of measures demonstrated some degree of correlation with pathological scores of disease progression including Braak staging (as reported above), but also with CERAD scores of plaque density (Table 2). All tau markers, both soluble and insoluble, reported relatively strong correlations with CERAD neuritic plaque score. Surprisingly, soluble but not insoluble (MOAB-2 reactive) Aβ correlated with the CERAD neuritic plaque score. Nevertheless, OC yielded a strong correlation with CERAD scores independent of fraction.

Measures of insoluble tau pathology (phosphorylation and oligomeric) largely mirrored the robust correlations previously reported between soluble tau pathology and cognitive scores (Koss et al., 2016). Total measures of insoluble tau via HT-7 failed to correlate with scores of any cognitive test examined here. Of the pathological markers, insoluble AT8 demonstrated the weakest correlation with cognition, with only modest relationships reported for MMSE and global CDR scores.

Comparable to the relationship between tau pathology and cognition in both fractions were only the data obtained for OC-reactive amyloid but not for measures of total Aβ as insoluble Aβ largely failed to correlate with cognitive scores (Table 2). As previously reported, soluble total Aβ pathology tracked strongly with disease progression and cognitive impairment (Koss et al., 2016 and Table 2).

To further resolve relations with insight into the earlier stages of the disease and in a bid to limit the impact of end stage data points, this analysis was also conducted across Braak stage 0-4, omitting Braak 5 and 6 pathology cases (see Table 2: values provided in brackets). The resulting correlations can be summarised as follows: 1. Measures of total tau failed to correlate with either Braak or CERAD neuropathological scores as well as any cognitive measures 2. Phospho- and oligomeric tau measures largely failed to report significant correlations with scales of cognitive assessment, despite preserved correlations with Braak staging; 3. Except for soluble total Aβ where correlative strength was largely unaffected, a similar loss of significance was observed for all other Aβ markers.

3. Discussion

This study reports on the relationship of soluble and insoluble tau and amyloid pathology from human temporal lobe samples in the context of neuropathological and cognitive measures of AD disease progression. Here, the direct comparison of soluble and insoluble AD markers largely supports and extends our previous findings that soluble pathology better tracks disease status and mental decline (Koss et al., 2016). Interestingly, two distinct profiles of solubility were observed: most markers displayed a coordinated rise of immunoreactivity in both soluble and insoluble preparations, but specifically, phospho-tau markers appeared to follow a lag phase of deposition, rising first in the soluble fraction. In

addition, the quantification of sequence-independent insoluble amyloid fibrils provided an improved measure of pathology, offering stronger correlations with disease progression as well as intellectual impairment compared to total levels of insoluble Aβ. Nevertheless, measures of tau pathology remained the strongest correlates of all aspects of the disease, when considered across all Braak stages, however only soluble total Aβ remained correlated with disease progression and impairment when end-stage cases were excluded.

3.1 Associations of soluble vs insoluble Tau species

Given that the quantification of AT8 histological immunoreactivity under the scheme of Braak staging is the principle measure of AD progression (Braak and Braak, 1995), it is unsurprising that multiple indices of tau pathology strongly tracked many measures of disease severity. Nevertheless, divergence amongst these tau markers in relation to progressive elevation and emergence within the insoluble fraction was evident.

All tau markers in the soluble fraction except for the oligomeric tau antibody were elevated in intermediate and high neuropathology cases compared to low controls. In contrast, no rise was seen in the intermediate cases for insoluble measures of total tau, CP13 and AT8 phospho-tau antibodies. The temporal emergence of insoluble tau pathology is in accordance with pathology of the superior temporal lobes, with NFTs at Braak stage 4 /5 (Alafuzoff et al., 2008) and the preceding elevation of soluble phospho-tau in line with the presence of pre-tangle neurons prior to the formation of mature aggregation (Braak et al., 2011). Indeed, supported by the detection of CP13 positive neurons which otherwise appear normal, even in non-demented cases (Kimura et al., 1996) we have previously reported that the CP13 phospho-epiptope may be an earlier marker of tau pathology (Koss et al., 2016).

Although single endpoint post-mortem studies cannot track progression of pathological tau species from soluble to insoluble compartments, our hypothesis is strongly supported by the age dependent translocation of specific phosphorylated tau species into insoluble aggregates in animal models (Delobel et al., 2008). Furthermore, the delayed deposition of insoluble tau species has been determined *in vitro* (Friedhoff et al., 1998). The lag phase for the production of insoluble tau species is in part a result of the net positive charge of the molecule, which makes the adoption of ordered protein structures such as β-sheets unfavourable, and requires conformational changes to an aggregation competent state (see Nizynski et al., 2017 for review).

Tau fibrillisation may require site-specific phosphorylation, as indicated here by measures of PHF1 reactive tau, which suggests differential kinetics compared to CP13 and AT8 reactive tau. PHF1 immunoreactivity rose simultaneously across both soluble and insoluble fractions and may imply that the phosphorylation of PHF1 residues (serine 396 and threonine 404) are facilitatory to the aggregation of insoluble tau species. Many pseudo-phosphorylation studies support differential promotion of tau aggregation via site directed phosphorylation, such that C-terminal phosphorylation promotes aggregation, whilst N-terminal

phosphorylation may inhibit or be benign for aggregation (Iqbal et al., 2009; Martin et al., 2011 for reviews). Accordingly, phospho-mimetic mutations at the PHF-1 epitope of tau displays enhanced aggregation kinetics in a number of *in vitro* assays (Ding et al., 2006; Abraha et al., 2000; Haase et al., 2004). Post mortem histological studies further support a prominent role for PHF1 in tau aggregation, i.e. early tau aggregates are more frequently labelled with PHF1 compared to AT8 (Mondragón-Rodriguez et al., 2014). Equally, sampling of the parahippocampal cortex reported on a subpopulation of PHF-1 positive yet AT-8 negative NFTs (Merino-Serrais et al., 2013).

An increased propensity for insoluble aggregation may also account for the parallel increase in soluble and insoluble oligomeric (TOC1) tau species in relation to Braak stages. Of note, significant elevations in TOC1 reactivity were only evident when comparing high to low neuropathological cases. Primarily reported to label dimeric tau species when resolved under non-denaturing conditions, electron micrographs have demonstrated the binding of TOC1 to a mixture of irregular shaped oligomers and the terminal ends of short filaments (Patterson et al., 2011; Ward et al., 2014). The end labelling of filaments may be indicative of TOC1 positive oligomers undergoing seeding and aggregation by oligomeric-nucleated conformation induction (Gerson and Kayed, 2013). Low-weight tau oligomers (dimers/trimers) are capable of promoting monomeric tau to form similar oligomers hence leading to fibrillization following prolonged incubations (Lasagna-Reeves et al., 2010+2012). However, previous characterisation of TOC1 reactive tau dimers have not been demonstrated to form fibrils without additional cofactors *in vitro* (Patterson et al., 2011). In human tissue TOC1 immunoreactivity did not co-localise with Thioflavin-S and Ab39 staining, two markers of mature tau aggregation (Ward et al., 2014). If indeed integrated into fibrils, TOC1 reactive structures may be masked within the aggregates and only emerge after solubilisation in formic acid. Nevertheless, soluble TOC1 positive tau species closely tracked the abundance of insoluble tau species hence offering support for the putative integration of TOC1 positive dimers into fibrils or other insoluble structures.

3.2 Measures of Amyloid

As with PHF1 and TOC1 reactive tau species, both total Aβ as well as fibrillary amyloid detected by MOAB-2 and OC antibodies, respectively, also demonstrated a progressive and parallel increase in the both fractions. Correlations suggest aggregation kinetics in line with *in vitro* studies where Aβ peptides readily aggregate at low concentrations (nM) in the absence of any co-factors (Vandersteen et al., 2012). Similarly, the rapid formation of OC competent oligomers and their maturation into OC reactive fibrils has been reported to occur in preparations of isolated $A\beta_{42}$ monomers (Coalier et al., 2013).

Consistent with many other studies, levels of both soluble and insoluble Aβ were elevated in AD cases compared to controls (McLean et al., 1999; Ingelsson et al., 2004; Tremblay et al., 2007). However, in contrast to the soluble fraction, insoluble Aβ (MOAB-2) measures

displayed a large degree of overlap between diagnosis groups and across neuropathological severity. Both histological (Price and Morris, 1999; Braak et al., 2011) and biochemical assessments (Tremblay et al., 2007; Maarouf et al., 2011) of post-mortem tissue reported high levels of variability, even many control cases presented with high levels of insoluble Aβ reactive material.

Improved diagnostic specificity, as offered by soluble MOAB reactive Aβ, was similarly observed by soluble OC reactive amyloid. Furthermore, OC quantification within the insoluble fraction demonstrated a reduced degree of overlap for both diagnosis and neuropathological severity stratification and improved correlative strength relative to disease progression and cognitive decline. The sequence independent OC antibody has been demonstrated to bind to a number of proteins, including Aβ, α-synuclein and islet amyloid polypetide but not tau aggregates such as NFTs at least within histological preparations (Kayed et al., 2007). The majority of immunoreactivity within the current samples therefore likely derives from interactions with Aβ. Nevertheless, given the heterogeneity of AD pathologies (McAleese et al., 2017; Walker et al., 2015) and the impact of technical factors related to tissue homogenisation, it cannot be ruled out that tau, α-synuclein and or TAR DNA-binding protein 43 may also have contributed to the overall signal. Previous work has reported a significant elevation in soluble OC reactive fibrillary oligomers in various regions of AD affected brains (Tomic et al., 2009) as also observed here. In the present study, we extend these findings reporting a similar increase in insoluble OC reactive material and strong correlative relationships with Braak and CERAD scores for both soluble and insoluble OC fibrils. Histological examination of AD mouse models suggests that the accumulation of soluble and insoluble OC reactive material is closely associated with plaque formation (Liu et al., 2015). The improved separation cf. diagnosis and neuropathological severity observed with insoluble measures of OC over MOAB-2 may indicate that only a subset of aggregates, i.e. those rich in OC reactive fibrils, may be associated with *bona fide* disease relevant pathology.

3.3 Correlation between pathological markers and cognitive scores

In agreement with previous histopathological (Arriagada et al., 1992; Giannakopoulos et al., 2003; Markesbery 2006) and biochemical studies (Näslund et al., 2000; Tremblay et al., 2007), our initial findings indicated superior associations between soluble vs. insoluble markers and MMSE and CDR scores. Furthermore, tau-based pathology more robustly correlated with cognitive impairment than Aβ, independent of solubility.

When considered across all Braak stages, all markers of tau pathology correlated to a varying degree with disease progression as well as with cognitive scores. However, levels of total insoluble tau (HT7) within the medial temporal gyrus failed to robustly track cognitive decline and insoluble measures of all tau markers reported a diminished relationship with ante-mortem cognition. The lack of predictive value of insoluble tau pathology is perhaps

unsurprising as numerous studies have reported the age-related deposition of tau within this area, without prominent cognitive impairment (Spires-Jones et al., 2017). Indeed, by 80 years of age ~50% of individuals demonstrate pathology consistent with a classification of Braak stage 3 or 4 (Braak et al., 2011).

A common feature of neuronal injury as well as aging, moderate tau pathology is observed following a variety of conditions with varying impact on cognitive faculties such as epilepsy (Thom et al., 2011) and subclinical chromic traumatic encephalopathy (McKee et al., 2012). This may further confound the relevance of broad-spectrum measures of tau in relation to cognitive decline. Accordingly, after exclusion of end stage cases with the highest levels of tau pathology, correlations between cognition and tau measures were lost.

Though in many cases levels of both soluble and insoluble Aβ are reportedly elevated in AD cases compared to controls, correlations with symptoms are rarely observed (McLean et al., 1999; Ingelsson et al., 2004; Tremblay et al., 2007). Tremblay and colleagues reported modest correlations of soluble and insoluble Aβ with cognitive scores, yet this was only specific to $A\beta_{42,}$ in contrast to our measures of total Aβ which tracked both cognitive scores and Braak staging. Here, the use of a N-terminal directed antibody (Youmans et al., 2012), rather than the frequently employed $A\beta_{40}$ or $A\beta_{42}$ C-terminal directed antibodies, may have provided improved specificity for the detection of a number of Aβ variants, potentially offering a more robust method of Aβ quantification. Nevertheless, insoluble measures of Aβ were weaker than the soluble measures, likely as a result of the extensive overlap of Aβ plaques seen between high pathological controls and demented individuals (Price and Morris, 1999).

The generalised fibril antibody OC yielded improved correlations with cognitive scores, Braak staging and CERAD scores particularly in the insoluble fraction when compared to total Aβ. The apparent improved relevance of insoluble OC may relate to the increased specificity of the antibody, which detects amyloid fibrils with toxic potential, in contrast to total Aβ measures which may be confounded by the additional detection of non-toxic aggregates. These findings extend previous analyses of soluble OC reactive fibrillary oligomers within the entorhinal and frontal cortex, aligned with MMSE, Thal phase and Braak staging (Tomic et al., 2009). Our data suggest that both soluble and insoluble pools of fibrillary amyloid correlate with disease progression as well as cognitive impairment, it remains however unclear which species and compartments are causative for neuronal dysfunction. It is conceivable that such measures may merely be indices of progressive amyloid pathology rather than the principle toxic forms. Indeed, many animal models have demonstrated improved specificity for the emergence and elevation of A11 reactive prefibrillar Aβ species in conjunction with behavioural deficits, over that of OC reactive species (Lefterov et al., 2009; Liu et al., 2015; Chiang et al., 2017).

Similar to that of tau pathology, measures of OC reactive species were dependent on late stage cases for correlation with cognitive decline and disease progression. In contrast

however soluble total Aβ remained highly correlated following the exclusion for end stage cases. The robustness of this relationship suggests soluble Aβ levels to be more indicative for early stage AD pathology than tau, at least in the temporal lobe.

3.4 Limitations

The current study is not without its limitations, most of which are relevant to post-mortem studies in general: Although the spread of tau and amyloid pathology is believed to represent a progressive scale, such a continuum cannot be thought of in relation to the diagnosis of AD. For moderate neuropathology cases (Braak stage 3 and 4), it is impossible to ascertain if such cases would have progressed to more advanced pathology and the ultimate diagnosis of AD. Hence, assumptions were made here regarding the progression of pathology between cases of likely differing status Similarly, the use of a single brain region (BA 21, lateral temporal cortex) precludes the generalisation of such relationships between soluble and insoluble pathology throughout the brain. Though relationships and equilibria are likely preserved across brain regions, a detailed multi-regional study is warranted. Furthermore, from post-mortem studies alone it is impossible to determine the causative contribution of each biochemically distinct species. These may merely be a consequence or by-product of degeneration, thus acting as a surrogate for neuronal injury potentially caused by other pathological cascades.

As with all antibody based studies, the detection and identification of distinct pathological species relies on the specificity of the antibodies, lysis conditions and sample preparations (Kumar et al., 2008). Many studies, including our own, have highlighted the potential for modification of Aβ oligomerisation and immunoreactivity due to experimental procedures (Hepler et al., 2006; Pujol-Pina et al., 2015; Koss et al., 2016). As yet, no systematic study has been conducted into the consequences of experimental parameters for the detection of tau oligomers, although for example, the post-mortem interval likely alters levels of phosphorylation (Ferrer et al., 2007). Here, we employed native state dot blots to minimise sample exposure to denaturing factors and thus preserve conformational states. However, this is not without its own issues, as immunoreactivity within individual dots may represent multiple molecular species, distinct in molecular weight, which cannot be distinguished. Therefore, the protein detection achieved by native state dot blots likely include truncation/degradation products which retain epitope competent sequences. A final consideration is that antigens may exist in alternative conformation/aggregation states in different lysis fractions, resulting in altered antibody affinity. This limitation is somewhat

addressed by reporting data relatively to controls within a specific fraction, although cross fractional comparison may be impacted due to varying antibody sensitivity.

The use of additional techniques such as ELISAs and mass spectrometry (MS) would allow for a more comprehensive profile of pathological proteomic changes to be reported. Specifically the characterisation of pathology would benefit from the determination of target protein species concentration rather than relatively changes from non-pathological conditions. A further advantage of MS is that it is not limited to target lead research and thus improves upon antibody based studies enabling the identification of unknown modifications and proteins within pathological tissue.

3.5 Conclusions

The present study builds upon prior post-mortem examination of AD brain tissue and serves to highlight different rates of tau and amyloid accumulation within the temporal lobe. The study provides evidence for site-directed tau phosphorylation and oligomerisation in promoting aggregation into insoluble structures. Equally, the quantification of selective Aβ species with established toxicity offers greater correlation with disease progression and cognitive decline than a generalised measure of Aβ, particularly within insoluble compartments whilst highlights soluble Aβ of potentially the most relevant to early stage changes.

4. Methods

4.1 Tissue samples

Human tissue and metadata for this current study were supplied by the MRC London Neurodegenerative Diseases Brain Bank, The Thomas Willis Oxford Brain Collection, The Manchester Brain Bank, the Newcastle Tissue Resource and the South West Dementia Brain Bank and was overall co-ordinated via the Brains for Dementia (BDR) initiative.

Human temporal cortex samples (n=46, middle temporal gyrus, Brodmann area 21) as previously reported (Koss et al., 2016) were used for the comparative investigation of AD relevant proteinopathy markers in NP40-lysis soluble and insoluble fractions. Samples were received as 500 mg frozen blocks and stored at -80^{o}C before processing. Metadata included gender, age at death, post-mortem interval (PMI), cortical pH (were recorded) as well as clinical diagnosis in relation to AD (non-AD or AD) and neuropathological assessments; Braak stage (n=46) and CERAD neuritic plaque score (n=35) in addition to cognitive scores from the Mini Mental State Exam (MMSE; n=43) and Clinical Dementia Rating (CDR) global (n=44), memory (n=44) and sum of box scores (n=34) variants. Those cases with a clinical diagnosis of AD and consistent neuropathology (Braak stage ≥4) were considered as AD cases, non-AD cases comprised of those without a clinical diagnosis of AD nor related dementia's and

whose neuropathological examination did not report any obviously signs of underlying neurological conditions. See Table 3 for summary.

4.2 Brain lysate preparation

Samples were processed as previously outlined (Koss et al., 2016). In brief, 100 mg of frozen tissue was manually homogenised in ~1:10 (w/v) modified NP-40/ Igepal based non-denaturing, non-ionic lysis buffer (in mM: 20 HEPES, 150 NaCl, 0.1 EDTA, 1% Igepal, p.H =7.6) containing complete protease inhibitor (Roche) and PhosStop tablets (Roche). Samples were cleared of insoluble material via centrifugation (13,000 g, 4^{O}C for 20mins) and supernatant collected as Igepal soluble material (referred to throughout as the *soluble fraction*). The resulting pellet was further homogenised twice in lysis buffer (1ml) and spun (13,000 g, 4^{O}C for 20mins) prior to resuspension and overnight incubation with agitation in 1:1 (w/v) 70% formic acid at 4^{O}C. The formic acid suspension was spun (18,000 g, 4^{O}C for 20mins) and the supernatant collected (referred to throughout as the *insoluble fractio*n) and stored at -80^{O}C. Prior to use the insoluble fraction was mixed in 4 volumes of neutralising buffer (2M Tris + 2M NaH_2PO_4).

4.3 Immuno-blots

For soluble fractions protein concentration was established via bicinchoninic acid assay (BCA, Sigma-Aldrich, Poole, UK) and adjusted to the desired concentration via sample dilution in lysis buffer. Due to the strong reducing action of formic acid the determination of protein concentration via standard protein quantification methods was not possible for the insoluble fraction and as such a set volume of neutralised samples was used. Nevertheless, all immuno-blot signals were adjusted via a Coomassie total protein stain (see below).

Both fractions were subject to standard Western blot and dot blot protocols (as described in Koss et al., 2016). For Western blotting, all samples were mixed with lithium dodecyl sulphate (LDS, Nupage, Thermo Fisher Scientific, Paisley, UK) and 15 mM dithiothreitol (DTT, Sigma), heated at 70^{O}C for 10mins prior to being run (20 µg/lane of soluble fraction and 10 µl/lane for neutralised insoluble samples) on 4-12% Bis-Tris precast gels (Nupage, Thermo Fisher Scientific). For Aβ and fibrillary amyloid detection, samples were separated for 35 mins in MES buffer and for tau for 45 mins in MOPS buffer at 200 V constant voltage. Proteins were then either transferred to 0.2 µm nitrocellulose membranes via the IBlot system, followed by microwaving for 3 mins in PBS or to 0.45 µm nitrocellulose membranes via standard transfer conditions for tau.

For dot blots, samples were dotted directly to 0.2 µm nitrocellulose membranes (5 µl of 2 µg/µl per dot for soluble and 5 µl of neutralised insoluble samples), without the addition of LDS or DTT or heating.

All blots were washed in 0.05% Tween-20 (Sigma) containing Tris-buffered saline (TBST, in mM; 50 Trizma base, 150 NaCl, pH=7.6) before being blocked for 1hr at room temperature in TBST containing 5% milk power and subsequently incubated overnight at 4^{O}C with the

relevant antibodies (see Table 4 for details) in 5 % bovine serum albumin containing TBST + 0.05 % Na-Azide (Sigma). Primary antibodies were labelled with appropriate secondary antibodies conjugated to horse radish peroxidase (1hr, room temperature in TBST + 5% milk powder + 1:5000, goat anti-rabbit or anti-mouse secondary antibodies IgG/ IgM isotypes). Immunoreactivity was visualised via enhanced chemiluminescence (1.25mM Luminol, 30µM coumaric acid and 0.015% H_20_2) and captured with use of a Vilber-Fusion- SL Camera (Vilber, Eberhardzell, Germany). The exposure time for each individual blot was determined by Fusion software (Vilber, Eberhardzell, Germany) auto-exposure function ensuring no pixel saturation. The resulting images were saved as 8 bit for illustration and 16 bit for quantification.

After capture of immunoreactivity, blots were processed for total protein following a standard Coomassie protein stain (as described previously Koss et al., 2016).

4.4 Immuno-blot quantification

ECL images and Coomassie labelled protein stains were quantified using area under curve (AUC) measurements as calculated by ImageJ (Ver 1.47, NIH, USA). ECL values were adjusted for total protein load as per Coomassie stained membranes and normalised within blots to one of three analytical classifications (also see Koss et al., 2016):

1. Post-mortem confirmed clinical diagnosis, eg. Non-AD cases (i.e. Braak 0-3) and AD cases (i.e. Braak 4-6). Normalisation conducted to mean intensity of Non-AD cases within blots.
2. Grouped Braak stages: low, intermediate and high severity of Braak pathology (Braak 0-2, Br 3-4 and Br 5-6, respectively). Normalisation conducted to mean intensity of low neuropathology cases within blots.
3. Individual Braak scores: cases separated into individual stages. Normalisation conducted to mean intensity of Braak stage 2 cases within blots.

4.5 Statistical analysis

All 46 human case samples were probed for all markers in both soluble and insoluble fraction-based dot blots. Samples were run in fixed batches (4 batches; containing 10-16 samples) and normalisation (as outlined above) conducted within blots, prior to pooling data between batches, such that all measures reported here are compiled from all cases. All statistical analysis was conducted using Graphpad Prism (ver 5.04). Normal distribution was probed via the Shaprio-Wilk test. Comparative analysis was subsequently preformed using either a Student's two tailed t test or its non-parametric equivalent (Mann-Whitney U test) to compare two data sets. Multiple group comparisons were performed via a 1-way analysis of variance (ANOVA) or Kruskal-Wallis ANOVA with selected post-hoc paired comparisons via Bonferroni or Dunn's test. Two variable multi-group comparisons were conducted using 2-way ANOVA and bonferroni post-tests where appropriate. Correlations were determined via Spearman's Rank correlation coefficient. Correlations presented in Table 1 and 2 were adjusted for multiple comparisons using a Bonferroni correction to α, i.e.

α=1-(1-0.005) and 1-(1-0.003571), respectively. In order to maintain consistency of statistical reporting e.g. ($p<0.05$), p values are reported as $1-(1-[p/10])^{10}$ and 1-(1-[p/14])14 in Table 1 and 2, respectively.

For correlations with Braak staging, significant outcomes were further probed via a one-tailed t-test to determine the initial stage for a significant deviation from pathology-free Braak 0 cases. For all analysis, $p<0.05$ was regarded as reliable with further statistical strength observed for $p<0.01$, $p<0.001$ and $p<0.0001$.

Figure legends

Figure 1. SDS page identification of distinct soluble and insoluble tau, Aβ and amyloid species. Example Western blot images resulting from probing of soluble (Sol) and insoluble (InSol) lysates from control (con) and AD cases with total tau antibody HT-7 (a), phospho-tau antibodies CP13 (b) and PHF1 (c), Aβ antibody MOAB (d) and the fibrillary amyloid antibody OC (e). Corresponding Braak stage (Br) classifications for each sample are shown above each lane and molecular weight marker with weights in kDa shown for orientation.

Figure 2. Soluble and insoluble tau. Soluble (Sol) and Insoluble (Insol) total tau (HT-7) dot blots **(i)** in cases labelled as Alzheimer's disease (AD) and control (C) cases and corresponding Braak stage (Br). Analysis of reactivity normalised to total protein stratified for **(ii)** diagnosis, neuropathology severity (**iii**, Low; Br 0-2, Intermediate (Inter); Br 3-4 and High; Br 5-6) and correlated with individual Br stage, with Spearman's correlation (r) reported in legend (**iv)**. Pooled data obtained from 4 independent batches of blots each with different cases (n=46 total) are presented as scatter plots and mean ± SEM in ii + iii and as mean + / - SEM in iv. Statistical significance is indicated as **=p<0.01, ***=p<0.001 and ****=p<0.01. $ denotes earliest Braak stage at which the signal is significantly elevated from pathology free cases (Br 0).

Figure 3. Soluble and insoluble phospho tau pathology; Soluble (Sol) and Insoluble (Insol) dot blots for AT8 (a), CP13 (b) and PHF-1 (c) reactive phospho tau **(i)**. Samples are indicated as Alzheimer's disease (AD) and control (C) cases with assigned Braak stage (Br). Immunoreactivity adjusted for total protein quantified according to diagnosis **(ii)**, neuropathology severity (**iii**, Low; Br 0-2, Intermediate (Inter); Br 3-4 and High; Br 5-6) and individual Br stage, Spearman's correlation (r) reported in legend (**iv)**. Scatter plots depict data obtained from 4 independent blots of cases run in batches (n=46 total cases). Mean ± SEM values are present in ii + iii and mean + / - SEM in iv. Statistical outcomes are denoted **=p<0.01, ***=p<0.001 and ****=p<0.0001. $ indicates the earliest Braak stage at which the signal is significantly elevated from pathology free cases (Br 0).

Figure 4. Soluble and insoluble oligomeric tau; Soluble (Sol) and Insoluble (Insol) dot blots for tau oligomeric complex 1 (TOC1) immunoreactivity **(i)**. Samples are indicated as Alzheimer's disease (AD) and control (C) cases with assigned Braak stage (Br). Quantified signal intensity normalised against total protein Coomassie stain shown as per diagnosis (**ii**), severity of neuropathology (iii; low; Br0-2, intermediate (inter); Br 3-4 and high; Br 5-6) and individual Braak stage (**iv**) stratifications. Data pooled from 4 blots containing different cases (n=46 total cases) presented as scatter plots with mean ±SEM (ii+iii)/ mean + or – SEM and Spearman's correlation (r) stated in the legend (iv). as **=p<0.01,***=p<0.001 and ****=p<0.0001. $ denotes the initial Braak stage at which quantified signal is significantly elevated from Braak stage 0.

Figure 5. Soluble and insoluble β amyloid; Dot blots for total Aβ stained with the MOAB-2 antibody. Alzheimer's disease (AD) and control (C) cases and corresponding Braak stage (Br) are indicated. Immunoreactivity adjusted for total protein as per Coomassie stain quantified according to diagnosis (**ii**), severity of neuropathology (iii; low; Br0-2, intermediate (inter); Br 3-4 and high; Br 5-6) and individual Braak stage (**iv**) is shown. Scatter plots of pooled data from 4 batches of blots (n=46 total

cases) with mean ±SEM indicated are presented in ii+iii and mean + or – SEM in iv with Spearman's correlation (r) noted in the legend. Statistical comparisons are indicated as *=p<0.05, ***=p<0.001 and ****=p<0.0001. $ denotes the initial Braak stage at which quantified signal is significantly elevated from Braak stage 0. NS = not significant.

Figure 6. Soluble and insoluble fibril amyloid; Soluble (Sol) and Insoluble (Insol) dot blots for amino acid sequence independent fibril amyloid as detected via the OC antibody. Cases are noted as Alzheimer's disease (AD) and control (C) cases alongside Braak stage (Br). Quantification of cohort as normalised to total protein and subsequently diagnosis (**ii**), severity of neuropathology (iii; low; Br0-2, intermediate (inter); Br 3-4 and high; Br 5-6) and individual Braak stage (**iv**) is shown. Individual normalised data for each case is presented in scatter plots (n=46 total cases) with mean ±SEM indicated in ii+iii and as Braak stage mean + or – SEM in iv with Spearman's correlation (r) noted in the legend. Statistical comparisons are indicated as *=p<0.05, **=p<0.01, ***=p<0.001 and ****=p<0.0001. $ denotes the initial Braak stage at which quantified signal is significantly elevated from Braak stage 0.

Table legends

Table 1: Correlation of tau and amyloid pathology. Correlation between soluble (sol) and insoluble (Insol) pathology. Spearman correlations (r) between measures of tau markers [Total tau (HT7), phospho-tau (AT8, CP13 and PHF1) and oligomeric tau (TOC1)] and amyloid markers [total Aβ (MOAB-2) and fibril amyloid (OC)] are reported. Significance (all p<0.05) are reported here was subject to bonferroni corrections for multiple comparisons. NS= not significant.

Table 2: Tau and amyloid pathology correlations with neuropathological staging schemes and cognitive scores. Soluble (s) and insoluble (I) tau [Total tau (HT7), phospho-tau (AT8, CP13 and PHF1) and oligomeric tau (TOC1)] and amyloid total Aβ (MOAB-2) and fibril amyloid (OC)] markers are presented. Spearman's rank correlations (r) between Braak staging and CERAD neuropathological scores as well as cognitive scores as assessed by the mini mental state exam (MMSE) and clinical dementia rating (CDR) alongside CDR memory and sum of boxes (SOB). Values given in brackets report correlations obtained following the exclusion of end stage Braak stage 5/6 pathological cases. Strength of statistical significance following bonferroni corrections for multiple comparisons are shown where *=p<0.05, **=p<0.01, ***=p<0.001 and ****=p<0.0001 and NS= not significant.

Table 3: Biographical and pathological data of cohort. Cases are organised according to analytical stratifications (diagnosis, neuropathological severity and individual Braak stage). CERAD neurtic plaque score, sample size (N), gender composition (% males) and the mean ± SEM and range of age, post-mortem interval (PMI) and cortical pH are provided.

Table 4 Antibodies. Commercial names, epitope, specificity, dilution and supplier are given for antibodies used in the study. Phospho-epitopes for antibodies are provide with phosphorylated (p) residues listed as either Serine (Ser) or Threonine (Thr), amino acid (aa) sequences given according to the longest isoform.

Acknowledgements

We would like to deeply thank all donors and their families for the tissue provided for this study. Human tissue samples were supplied by the Brains for Dementia Research programme, jointly funded by Alzheimer's Research UK, the Alzheimer's Society and the Medical Research Council, and sourced from the MRC London Neurodegenerative Diseases Brain Bank, the Manchester Brain Bank, the South West Dementia Brain Bank (SWDBB), the Newcastle Brain Tissue Resource and the Oxford Brain Bank. The Newcastle Brain Tissue Resource and Oxford Brain Bank are also supported by the National Institute for Health Research (NIHR) Units. The South West Dementia Brain Bank (SWDBB) receives additional support from BRACE (Bristol Research into Alzheimer's and Care of the Elderly). Antibodies CP13 and PHF1 were generously provided by Prof Peter Davies. TOC1 antibodies were a gift from Nicholas Kanaan at Michigan State University (originally created by Lester Binder at Northwestern University).

Funding

The work presented here was funded by Alzheimer's Research UK (Grant refs: ARUK-PPG2014A-21, ARUK-NSG2015-1 and ARUK-NCG2017A-3 to BP and DK).

References

ABRAHA, A., GHOSHAL, N., GAMBLIN, T.C., CRYNS, V., BERRY, R.W., KURET, J. and BINDER, L.I., 2000. C-terminal inhibition of tau assembly in vitro and in Alzheimer's disease. *Journal of cell science,* **113 Pt 21**, pp. 3737-3745.

ALAFUZOFF, I., ARZBERGER, T., AL-SARRAJ, S., BODI, I., BOGDANOVIC, N., BRAAK, H., BUGIANI, O., DEL-TREDICI, K., FERRER, I., GELPI, E., GIACCONE, G., GRAEBER, M.B., INCE, P., KAMPHORST, W., KING, A., KORKOLOPOULOU, P., KOVACS, G.G., LARIONOV, S., MEYRONET, D., MONORANU, C., PARCHI, P., PATSOURIS, E., ROGGENDORF, W., SEILHEAN, D., TAGLIAVINI, F., STADELMANN, C., STREICHENBERGER, N., THAL, D.R., WHARTON, S.B. and KRETZSCHMAR, H., 2008. Staging of neurofibrillary pathology in Alzheimer's disease: a study of the BrainNet Europe Consortium. *Brain pathology (Zurich, Switzerland),* **18**(4), pp. 484-496.

ARRIAGADA, P.V., GROWDON, J.H., HEDLEY-WHYTE, E.T. and HYMAN, B.T., 1992. Neurofibrillary tangles but not senile plaques parallel duration and severity of Alzheimer's disease. *Neurology,* **42**(3 Pt 1), pp. 631-639.

BECKETT, T.L., WEBB, R.L., NIEDOWICZ, D.M., HOLLER, C.J., MATVEEV, S., BAIG, I., LEVINE, H.,3RD, KELLER, J.N. and MURPHY, M.P., 2012. Postmortem Pittsburgh Compound B (PiB) binding increases with Alzheimer's disease progression. *Journal of Alzheimer's disease : JAD,* **32**(1), pp. 127-138.

BIESCHKE, J., HERBST, M., WIGLENDA, T., FRIEDRICH, R.P., BOEDDRICH, A., SCHIELE, F., KLECKERS, D., LOPEZ DEL AMO, J.M., GRUNING, B.A., WANG, Q., SCHMIDT, M.R., LURZ, R., ANWYL, R., SCHNOEGL, S., FANDRICH, M., FRANK, R.F., REIF, B., GUNTHER, S., WALSH, D.M. and WANKER, E.E., 2011. Small-molecule conversion of toxic oligomers to nontoxic beta-sheet-rich amyloid fibrils. *Nature chemical biology,* **8**(1), pp. 93-101.

BOLUDA, S., TOLEDO, J.B., IRWIN, D.J., RAIBLE, K.M., BYRNE, M.D., LEE, E.B., LEE, V.M. and TROJANOWSKI, J.Q., 2014. A comparison of Abeta amyloid pathology staging systems and correlation with clinical diagnosis. *Acta Neuropathologica,* **128**(4), pp. 543-550.

BRAAK, H. and BRAAK, E., 1995. Staging of Alzheimer's disease-related neurofibrillary changes. *Neurobiology of aging,* **16**(3), pp. 271-8; discussion 278-84.

BRAAK, H., THAL, D.R., GHEBREMEDHIN, E. and DEL TREDICI, K., 2011. Stages of the pathologic process in Alzheimer disease: age categories from 1 to 100 years. *Journal of neuropathology and experimental neurology,* **70**(11), pp. 960-969.

BRIER, M.R., GORDON, B., FRIEDRICHSEN, K., MCCARTHY, J., STERN, A., CHRISTENSEN, J., OWEN, C., ALDEA, P., SU, Y., HASSENSTAB, J., CAIRNS, N.J., HOLTZMAN, D.M., FAGAN, A.M., MORRIS, J.C., BENZINGER, T.L. and ANCES, B.M., 2016. Tau and Abeta imaging, CSF measures, and cognition in Alzheimer's disease. *Science translational medicine,* **8**(338), pp. 338ra66.

BURDICK, D., SOREGHAN, B., KWON, M., KOSMOSKI, J., KNAUER, M., HENSCHEN, A., YATES, J., COTMAN, C. and GLABE, C., 1992. Assembly and aggregation properties of synthetic Alzheimer's A4/beta amyloid peptide analogs. *The Journal of biological chemistry,* **267**(1), pp. 546-554.

CASTILLO-CARRANZA, D.L., GERSON, J.E., SENGUPTA, U., GUERRERO-MUNOZ, M.J., LASAGNA-REEVES, C.A. and KAYED, R., 2014. Specific targeting of tau oligomers in Htau mice prevents cognitive impairment and tau toxicity following injection with brain-derived tau oligomeric seeds. *Journal of Alzheimer's disease : JAD,* **40 Suppl 1**, pp. S97-S111.

CHIANG, A.C.A., FOWLER, S.W., REDDY, R., PLETNIKOVA, O., TRONCOSO, J.C., SHERMAN, M.A., LESNE, S.E. and JANKOWSKY, J.L., 2018. Discrete Pools of Oligomeric Amyloid-beta Track with

Spatial Learning Deficits in a Mouse Model of Alzheimer Amyloidosis. *The American journal of pathology,* **188**(3), pp. 739-756.

COALIER, K.A., PARANJAPE, G.S., KARKI, S. and NICHOLS, M.R., 2013. Stability of early-stage amyloid-beta(1-42) aggregation species. *Biochimica et biophysica acta,* **1834**(1), pp. 65-70.

COWAN, C.M., QURAISHE, S., HANDS, S., SEALEY, M., MAHAJAN, S., ALLAN, D.W. and MUDHER, A., 2015. Rescue from tau-induced neuronal dysfunction produces insoluble tau oligomers. *Scientific reports,* **5**, pp. 17191.

COX, K., COMBS, B., ABDELMESIH, B., MORFINI, G., BRADY, S.T. and KANAAN, N.M., 2016. Analysis of isoform-specific tau aggregates suggests a common toxic mechanism involving similar pathological conformations and axonal transport inhibition. *Neurobiology of aging,* **47**, pp. 113-126.

CRARY, J.F., TROJANOWSKI, J.Q., SCHNEIDER, J.A., ABISAMBRA, J.F., ABNER, E.L., ALAFUZOFF, I., ARNOLD, S.E., ATTEMS, J., BEACH, T.G., BIGIO, E.H., CAIRNS, N.J., DICKSON, D.W., GEARING, M., GRINBERG, L.T., HOF, P.R., HYMAN, B.T., JELLINGER, K., JICHA, G.A., KOVACS, G.G., KNOPMAN, D.S., KOFLER, J., KUKULL, W.A., MACKENZIE, I.R., MASLIAH, E., MCKEE, A., MONTINE, T.J., MURRAY, M.E., NELTNER, J.H., SANTA-MARIA, I., SEELEY, W.W., SERRANO-POZO, A., SHELANSKI, M.L., STEIN, T., TAKAO, M., THAL, D.R., TOLEDO, J.B., TRONCOSO, J.C., VONSATTEL, J.P., WHITE, C.L.,3RD, WISNIEWSKI, T., WOLTJER, R.L., YAMADA, M. and NELSON, P.T., 2014. Primary age-related tauopathy (PART): a common pathology associated with human aging. *Acta Neuropathologica,* **128**(6), pp. 755-766.

DELOBEL, P., LAVENIR, I., FRASER, G., INGRAM, E., HOLZER, M., GHETTI, B., SPILLANTINI, M.G., CROWTHER, R.A. and GOEDERT, M., 2008. Analysis of tau phosphorylation and truncation in a mouse model of human tauopathy. *The American journal of pathology,* **172**(1), pp. 123-131.

DING, H., MATTHEWS, T.A. and JOHNSON, G.V., 2006. Site-specific phosphorylation and caspase cleavage differentially impact tau-microtubule interactions and tau aggregation. *The Journal of biological chemistry,* **281**(28), pp. 19107-19114.

FERRER, I., SANTPERE, G., ARZBERGER, T., BELL, J., BLANCO, R., BOLUDA, S., BUDKA, H., CARMONA, M., GIACCONE, G., KREBS, B., LIMIDO, L., PARCHI, P., PUIG, B., STRAMMIELLO, R., STROBEL, T. and KRETZSCHMAR, H., 2007. Brain protein preservation largely depends on the postmortem storage temperature: implications for study of proteins in human neurologic diseases and management of brain banks: a BrainNet Europe Study. *Journal of neuropathology and experimental neurology,* **66**(1), pp. 35-46.

FODERO-TAVOLETTI, M.T., FURUMOTO, S., TAYLOR, L., MCLEAN, C.A., MULLIGAN, R.S., BIRCHALL, I., HARADA, R., MASTERS, C.L., YANAI, K., KUDO, Y., ROWE, C.C., OKAMURA, N. and VILLEMAGNE, V.L., 2014. Assessing THK523 selectivity for tau deposits in Alzheimer's disease and non-Alzheimer's disease tauopathies. *Alzheimer's research & therapy,* **6**(1), pp. 11.

FODERO-TAVOLETTI, M.T., OKAMURA, N., FURUMOTO, S., MULLIGAN, R.S., CONNOR, A.R., MCLEAN, C.A., CAO, D., RIGOPOULOS, A., CARTWRIGHT, G.A., O'KEEFE, G., GONG, S., ADLARD, P.A., BARNHAM, K.J., ROWE, C.C., MASTERS, C.L., KUDO, Y., CAPPAI, R., YANAI, K. and VILLEMAGNE, V.L., 2011. 18F-THK523: a novel in vivo tau imaging ligand for Alzheimer's disease. *Brain : a journal of neurology,* **134**(Pt 4), pp. 1089-1100.

FRIEDHOFF, P., SCHNEIDER, A., MANDELKOW, E.M. and MANDELKOW, E., 1998. Rapid assembly of Alzheimer-like paired helical filaments from microtubule-associated protein tau monitored by fluorescence in solution. *Biochemistry,* **37**(28), pp. 10223-10230.

GERSON, J.E. and KAYED, R., 2013. Formation and propagation of tau oligomeric seeds. *Frontiers in neurology,* **4**, pp. 93.

GIANNAKOPOULOS, P., HERRMANN, F.R., BUSSIERE, T., BOURAS, C., KOVARI, E., PERL, D.P., MORRISON, J.H., GOLD, G. and HOF, P.R., 2003. Tangle and neuron numbers, but not amyloid load, predict cognitive status in Alzheimer's disease. *Neurology,* **60**(9), pp. 1495-1500.

HAASE, C., STIELER, J.T., ARENDT, T. and HOLZER, M., 2004. Pseudophosphorylation of tau protein alters its ability for self-aggregation. *Journal of neurochemistry,* **88**(6), pp. 1509-1520.

HALVERSON, K., FRASER, P.E., KIRSCHNER, D.A. and LANSBURY, P.T.,JR, 1990. Molecular determinants of amyloid deposition in Alzheimer's disease: conformational studies of synthetic beta-protein fragments. *Biochemistry,* **29**(11), pp. 2639-2644.

HAN, P., SERRANO, G., BEACH, T.G., CASELLI, R.J., YIN, J., ZHUANG, N. and SHI, J., 2017. A Quantitative Analysis of Brain Soluble Tau and the Tau Secretion Factor. *Journal of neuropathology and experimental neurology,* **76**(1), pp. 44-51.

HANGER, D.P., BRION, J.P., GALLO, J.M., CAIRNS, N.J., LUTHERT, P.J. and ANDERTON, B.H., 1991. Tau in Alzheimer's disease and Down's syndrome is insoluble and abnormally phosphorylated. *The Biochemical journal,* **275 (Pt 1)**(Pt 1), pp. 99-104.

HAROUTUNIAN, V., DAVIES, P., VIANNA, C., BUXBAUM, J.D. and PUROHIT, D.P., 2007. Tau protein abnormalities associated with the progression of alzheimer disease type dementia. *Neurobiology of aging,* **28**(1), pp. 1-7.

HEPLER, R.W., GRIMM, K.M., NAHAS, D.D., BREESE, R., DODSON, E.C., ACTON, P., KELLER, P.M., YEAGER, M., WANG, H., SHUGHRUE, P., KINNEY, G. and JOYCE, J.G., 2006. Solution state characterization of amyloid beta-derived diffusible ligands. *Biochemistry,* **45**(51), pp. 15157-15167.

INGELSSON, M., FUKUMOTO, H., NEWELL, K.L., GROWDON, J.H., HEDLEY-WHYTE, E.T., FROSCH, M.P., ALBERT, M.S., HYMAN, B.T. and IRIZARRY, M.C., 2004. Early Abeta accumulation and progressive synaptic loss, gliosis, and tangle formation in AD brain. *Neurology,* **62**(6), pp. 925-931.

IQBAL, K., LIU, F., GONG, C.X., ALONSO ADEL, C. and GRUNDKE-IQBAL, I., 2009. Mechanisms of tau-induced neurodegeneration. *Acta Neuropathologica,* **118**(1), pp. 53-69.

JICHA, G.A., LANE, E., VINCENT, I., OTVOS, L.,JR, HOFFMANN, R. and DAVIES, P., 1997. A conformation- and phosphorylation-dependent antibody recognizing the paired helical filaments of Alzheimer's disease. *Journal of neurochemistry,* **69**(5), pp. 2087-2095.

JOSEPHS, K.A., MURRAY, M.E., TOSAKULWONG, N., WHITWELL, J.L., KNOPMAN, D.S., MACHULDA, M.M., WEIGAND, S.D., BOEVE, B.F., KANTARCI, K., PETRUCELLI, L., LOWE, V.J., JACK, C.R.,JR, PETERSEN, R.C., PARISI, J.E. and DICKSON, D.W., 2017. Tau aggregation influences cognition and hippocampal atrophy in the absence of beta-amyloid: a clinico-imaging-pathological study of primary age-related tauopathy (PART). *Acta Neuropathologica,* **133**(5), pp. 705-715.

JULIEN, C., BRETTEVILLE, A. and PLANEL, E., 2012. Biochemical isolation of insoluble tau in transgenic mouse models of tauopathies. *Methods in molecular biology (Clifton, N.J.),* **849**, pp. 473-491.

KANTARCI, K., LOWE, V., PRZYBELSKI, S.A., WEIGAND, S.D., SENJEM, M.L., IVNIK, R.J., PREBOSKE, G.M., ROBERTS, R., GEDA, Y.E., BOEVE, B.F., KNOPMAN, D.S., PETERSEN, R.C. and JACK, C.R.,JR, 2012. APOE modifies the association between Abeta load and cognition in cognitively normal older adults. *Neurology,* **78**(4), pp. 232-240.

KAYED, R., CANTO, I., BREYDO, L., RASOOL, S., LUKACSOVICH, T., WU, J., ALBAY, R.,3RD, PENSALFINI, A., YEUNG, S., HEAD, E., MARSH, J.L. and GLABE, C., 2010. Conformation dependent monoclonal antibodies distinguish different replicating strains or conformers of prefibrillar Abeta oligomers. *Molecular neurodegeneration,* **5**, pp. 57-1326-5-57.

KIMURA, T., ONO, T., TAKAMATSU, J., YAMAMOTO, H., IKEGAMI, K., KONDO, A., HASEGAWA, M., IHARA, Y., MIYAMOTO, E. and MIYAKAWA, T., 1996. Sequential changes of tau-site-specific phosphorylation during development of paired helical filaments. *Dementia (Basel, Switzerland),* **7**(4), pp. 177-181.

KOSS, D.J., JONES, G., CRANSTON, A., GARDNER, H., KANAAN, N.M. and PLATT, B., 2016. Soluble pre-fibrillar tau and beta-amyloid species emerge in early human Alzheimer's disease and track disease progression and cognitive decline. *Acta Neuropathologica,* **132**(6), pp. 875-895.

KSIEZAK-REDING, H., LIU, W.K. and YEN, S.H., 1992. Phosphate analysis and dephosphorylation of modified tau associated with paired helical filaments. *Brain research,* **597**(2), pp. 209-219.

KUCHIBHOTLA, K.V., WEGMANN, S., KOPEIKINA, K.J., HAWKES, J., RUDINSKIY, N., ANDERMANN, M.L., SPIRES-JONES, T.L., BACSKAI, B.J. and HYMAN, B.T., 2014. Neurofibrillary tangle-bearing neurons are functionally integrated in cortical circuits in vivo. *Proceedings of the National Academy of Sciences of the United States of America,* **111**(1), pp. 510-514.

KUMAR, S., RAVI, V.K. and SWAMINATHAN, R., 2008. How do surfactants and DTT affect the size, dynamics, activity and growth of soluble lysozyme aggregates? *The Biochemical journal,* **415**(2), pp. 275-288.

KURET, J., CHIRITA, C.N., CONGDON, E.E., KANNANAYAKAL, T., LI, G., NECULA, M., YIN, H. and ZHONG, Q., 2005. Pathways of tau fibrillization. *Biochimica et biophysica acta,* **1739**(2-3), pp. 167-178.

LASAGNA-REEVES, C.A., CASTILLO-CARRANZA, D.L., SENGUPTA, U., CLOS, A.L., JACKSON, G.R. and KAYED, R., 2011. Tau oligomers impair memory and induce synaptic and mitochondrial dysfunction in wild-type mice. *Molecular neurodegeneration,* **6**, pp. 39-1326-6-39.

LASAGNA-REEVES, C.A., CASTILLO-CARRANZA, D.L., SENGUPTA, U., SARMIENTO, J., TRONCOSO, J., JACKSON, G.R. and KAYED, R., 2012. Identification of oligomers at early stages of tau aggregation in Alzheimer's disease. *FASEB journal : official publication of the Federation of American Societies for Experimental Biology,* **26**(5), pp. 1946-1959.

LEFTEROV, I., FITZ, N.F., CRONICAN, A., LEFTEROV, P., STAUFENBIEL, M. and KOLDAMOVA, R., 2009. Memory deficits in APP23/Abca1+/- mice correlate with the level of Abeta oligomers. *ASN neuro,* **1**(2), pp. 10.1042/AN20090015.

MAAROUF, C.L., DAUGS, I.D., KOKJOHN, T.A., WALKER, D.G., HUNTER, J.M., KRUCHOWSKY, J.C., WOLTJER, R., KAYE, J., CASTANO, E.M., SABBAGH, M.N., BEACH, T.G. and ROHER, A.E., 2011. Alzheimer's disease and non-demented high pathology control nonagenarians: comparing and contrasting the biochemistry of cognitively successful aging. *PloS one,* **6**(11), pp. e27291.

MANDLER, M., WALKER, L., SANTIC, R., HANSON, P., UPADHAYA, A.R., COLLOBY, S.J., MORRIS, C.M., THAL, D.R., THOMAS, A.J., SCHNEEBERGER, A. and ATTEMS, J., 2014. Pyroglutamylated amyloid-beta is associated with hyperphosphorylated tau and severity of Alzheimer's disease. *Acta Neuropathologica,* **128**(1), pp. 67-79.

MARKESBERY, W.R., SCHMITT, F.A., KRYSCIO, R.J., DAVIS, D.G., SMITH, C.D. and WEKSTEIN, D.R., 2006. Neuropathologic substrate of mild cognitive impairment. *Archives of Neurology,* **63**(1), pp. 38-46.

MARTIN, L., LATYPOVA, X. and TERRO, F., 2011. Post-translational modifications of tau protein: implications for Alzheimer's disease. *Neurochemistry international,* **58**(4), pp. 458-471.

MATSUO, E.S., SHIN, R.W., BILLINGSLEY, M.L., VAN DEVOORDE, A., O'CONNOR, M., TROJANOWSKI, J.Q. and LEE, V.M., 1994. Biopsy-derived adult human brain tau is phosphorylated at many of the same sites as Alzheimer's disease paired helical filament tau. *Neuron,* **13**(4), pp. 989-1002.

MATVEEV, S.V., SPIELMANN, H.P., METTS, B.M., CHEN, J., ONONO, F., ZHU, H., SCHEFF, S.W., WALKER, L.C. and LEVINE, H.,3RD, 2014. A distinct subfraction of Abeta is responsible for the high-affinity Pittsburgh compound B-binding site in Alzheimer's disease brain. *Journal of neurochemistry,* **131**(3), pp. 356-368.

MCALEESE, K.E., WALKER, L., ERSKINE, D., THOMAS, A.J., MCKEITH, I.G. and ATTEMS, J., 2017. TDP-43 pathology in Alzheimer's disease, dementia with Lewy bodies and ageing. *Brain pathology (Zurich, Switzerland),* **27**(4), pp. 472-479.

MCKEE, A.C., STERN, R.A., NOWINSKI, C.J., STEIN, T.D., ALVAREZ, V.E., DANESHVAR, D.H., LEE, H.S., WOJTOWICZ, S.M., HALL, G., BAUGH, C.M., RILEY, D.O., KUBILUS, C.A., CORMIER, K.A., JACOBS, M.A., MARTIN, B.R., ABRAHAM, C.R., IKEZU, T., REICHARD, R.R., WOLOZIN, B.L., BUDSON, A.E., GOLDSTEIN, L.E., KOWALL, N.W. and CANTU, R.C., 2013. The spectrum of disease in chronic traumatic encephalopathy. *Brain : a journal of neurology,* **136**(Pt 1), pp. 43-64.

MCLEAN, C.A., CHERNY, R.A., FRASER, F.W., FULLER, S.J., SMITH, M.J., BEYREUTHER, K., BUSH, A.I. and MASTERS, C.L., 1999. Soluble pool of Abeta amyloid as a determinant of severity of neurodegeneration in Alzheimer's disease. *Annals of Neurology,* **46**(6), pp. 860-866.

MERINO-SERRAIS, P., BENAVIDES-PICCIONE, R., BLAZQUEZ-LLORCA, L., KASTANAUSKAITE, A., RABANO, A., AVILA, J. and DEFELIPE, J., 2013. The influence of phospho-tau on dendritic spines of cortical pyramidal neurons in patients with Alzheimer's disease. *Brain : a journal of neurology,* **136**(Pt 6), pp. 1913-1928.

MONDRAGON-RODRIGUEZ, S., PERRY, G., LUNA-MUNOZ, J., ACEVEDO-AQUINO, M.C. and WILLIAMS, S., 2014. Phosphorylation of tau protein at sites Ser(396-404) is one of the earliest events in Alzheimer's disease and Down syndrome. *Neuropathology and applied neurobiology,* **40**(2), pp. 121-135.

MUFSON, E.J., MALEK-AHMADI, M., SNYDER, N., AUSDEMORE, J., CHEN, K. and PEREZ, S.E., 2016. Braak stage and trajectory of cognitive decline in noncognitively impaired elders. *Neurobiology of aging,* **43**, pp. 101-110.

MUKAETOVA-LADINSKA, E.B., HARRINGTON, C.R., ROTH, M. and WISCHIK, C.M., 1993. Biochemical and anatomical redistribution of tau protein in Alzheimer's disease. *The American journal of pathology,* **143**(2), pp. 565-578.

NASLUND, J., HAROUTUNIAN, V., MOHS, R., DAVIS, K.L., DAVIES, P., GREENGARD, P. and BUXBAUM, J.D., 2000. Correlation between elevated levels of amyloid beta-peptide in the brain and cognitive decline. *Jama,* **283**(12), pp. 1571-1577.

NIZYNSKI, B., DZWOLAK, W. and NIEZNANSKI, K., 2017. Amyloidogenesis of Tau protein. *Protein science : a publication of the Protein Society,* **26**(11), pp. 2126-2150.

PATTERSON, K.R., REMMERS, C., FU, Y., BROOKER, S., KANAAN, N.M., VANA, L., WARD, S., REYES, J.F., PHILIBERT, K., GLUCKSMAN, M.J. and BINDER, L.I., 2011. Characterization of prefibrillar Tau oligomers in vitro and in Alzheimer disease. *The Journal of biological chemistry,* **286**(26), pp. 23063-23076.

PRICE, J.L. and MORRIS, J.C., 1999. Tangles and plaques in nondemented aging and "preclinical" Alzheimer's disease. *Annals of Neurology,* **45**(3), pp. 358-368.

PUJOL-PINA, R., VILAPRINYO-PASCUAL, S., MAZZUCATO, R., ARCELLA, A., VILASECA, M., OROZCO, M. and CARULLA, N., 2015. SDS-PAGE analysis of Abeta oligomers is disserving research into Alzheimer s disease: appealing for ESI-IM-MS. *Scientific reports,* **5**, pp. 14809.

RENTZ, D.M., AMARIGLIO, R.E., BECKER, J.A., FREY, M., OLSON, L.E., FRISHE, K., CARMASIN, J., MAYE, J.E., JOHNSON, K.A. and SPERLING, R.A., 2011. Face-name associative memory performance is related to amyloid burden in normal elderly. *Neuropsychologia,* **49**(9), pp. 2776-2783.

RIJAL UPADHAYA, A., KOSTERIN, I., KUMAR, S., VON ARNIM, C.A., YAMAGUCHI, H., FANDRICH, M., WALTER, J. and THAL, D.R., 2014. Biochemical stages of amyloid-beta peptide aggregation and accumulation in the human brain and their association with symptomatic and pathologically preclinical Alzheimer's disease. *Brain : a journal of neurology,* **137**(Pt 3), pp. 887-903.

ROSTAGNO, A. and GHISO, J., 2009. Isolation and biochemical characterization of amyloid plaques and paired helical filaments. *Current protocols in cell biology,* **Chapter 3**, pp. Unit 3.33 3.33.1-33.

RUGGERI, F.S., ADAMCIK, J., JEONG, J.S., LASHUEL, H.A., MEZZENGA, R. and DIETLER, G., 2015. Influence of the beta-sheet content on the mechanical properties of aggregates during amyloid fibrillization. *Angewandte Chemie (International ed.in English),* **54**(8), pp. 2462-2466.

SANCHEZ-MEJIAS, E., NAVARRO, V., JIMENEZ, S., SANCHEZ-MICO, M., SANCHEZ-VARO, R., NUNEZ-DIAZ, C., TRUJILLO-ESTRADA, L., DAVILA, J.C., VIZUETE, M., GUTIERREZ, A. and VITORICA, J., 2016. Soluble phospho-tau from Alzheimer's disease hippocampus drives microglial degeneration. *Acta Neuropathologica,* **132**(6), pp. 897-916.

SANTACRUZ, K., LEWIS, J., SPIRES, T., PAULSON, J., KOTILINEK, L., INGELSSON, M., GUIMARAES, A., DETURE, M., RAMSDEN, M., MCGOWAN, E., FORSTER, C., YUE, M., ORNE, J., JANUS, C., MARIASH, A., KUSKOWSKI, M., HYMAN, B., HUTTON, M. and ASHE, K.H., 2005. Tau suppression in a neurodegenerative mouse model improves memory function. *Science (New York, N.Y.),* **309**(5733), pp. 476-481.

SERPELL, L.C., 2000. Alzheimer's amyloid fibrils: structure and assembly. *Biochimica et biophysica acta,* **1502**(1), pp. 16-30.

SHAROAR, M.G., THAPA, A., SHAHNAWAZ, M., RAMASAMY, V.S., WOO, E.R., SHIN, S.Y. and PARK, I.S., 2012. Keampferol-3-O-rhamnoside abrogates amyloid beta toxicity by modulating monomers and remodeling oligomers and fibrils to non-toxic aggregates. *Journal of Biomedical Science,* **19**, pp. 104-0127-19-104.

SPIRES-JONES, T.L., ATTEMS, J. and THAL, D.R., 2017. Interactions of pathological proteins in neurodegenerative diseases. *Acta Neuropathologica,* **134**(2), pp. 187-205.

THAL, D.R., RUB, U., ORANTES, M. and BRAAK, H., 2002. Phases of A beta-deposition in the human brain and its relevance for the development of AD. *Neurology,* **58**(12), pp. 1791-1800.

THOM, M., LIU, J.Y., THOMPSON, P., PHADKE, R., NARKIEWICZ, M., MARTINIAN, L., MARSDON, D., KOEPP, M., CABOCLO, L., CATARINO, C.B. and SISODIYA, S.M., 2011. Neurofibrillary tangle pathology and Braak staging in chronic epilepsy in relation to traumatic brain injury and hippocampal sclerosis: a post-mortem study. *Brain : a journal of neurology,* **134**(Pt 10), pp. 2969-2981.

TOMIC, J.L., PENSALFINI, A., HEAD, E. and GLABE, C.G., 2009. Soluble fibrillar oligomer levels are elevated in Alzheimer's disease brain and correlate with cognitive dysfunction. *Neurobiology of disease,* **35**(3), pp. 352-358.

TREMBLAY, C., PILOTE, M., PHIVILAY, A., EMOND, V., BENNETT, D.A. and CALON, F., 2007. Biochemical characterization of Abeta and tau pathologies in mild cognitive impairment and Alzheimer's disease. *Journal of Alzheimer's disease : JAD,* **12**(4), pp. 377-390.

VANDERSTEEN, A., HUBIN, E., SARROUKH, R., DE BAETS, G., SCHYMKOWITZ, J., ROUSSEAU, F., SUBRAMANIAM, V., RAUSSENS, V., WENSCHUH, H., WILDEMANN, D. and BROERSEN, K., 2012. A comparative analysis of the aggregation behavior of amyloid-beta peptide variants. *FEBS letters,* **586**(23), pp. 4088-4093.

WALKER, L., MCALEESE, K.E., THOMAS, A.J., JOHNSON, M., MARTIN-RUIZ, C., PARKER, C., COLLOBY, S.J., JELLINGER, K. and ATTEMS, J., 2015. Neuropathologically mixed Alzheimer's and Lewy body disease: burden of pathological protein aggregates differs between clinical phenotypes. *Acta Neuropathologica,* **129**(5), pp. 729-748.

WALSH, D.M. and SELKOE, D.J., 2007. A beta oligomers - a decade of discovery. *Journal of neurochemistry,* **101**(5), pp. 1172-1184.

WANG, J., DICKSON, D.W., TROJANOWSKI, J.Q. and LEE, V.M., 1999. The levels of soluble versus insoluble brain Abeta distinguish Alzheimer's disease from normal and pathologic aging. *Experimental neurology,* **158**(2), pp. 328-337.

WARD, S.M., HIMMELSTEIN, D.S., REN, Y., FU, Y., YU, X.W., ROBERTS, K., BINDER, L.I. and SAHARA, N., 2014. TOC1: a valuable tool in assessing disease progression in the rTg4510 mouse model of tauopathy. *Neurobiology of disease,* **67**, pp. 37-48.

YOUMANS, K.L., TAI, L.M., KANEKIYO, T., STINE, W.B.,JR, MICHON, S.C., NWABUISI-HEATH, E., MANELLI, A.M., FU, Y., RIORDAN, S., EIMER, W.A., BINDER, L., BU, G., YU, C., HARTLEY, D.M. and LADU, M.J., 2012. Intraneuronal Abeta detection in 5xFAD mice by a new Abeta-specific antibody. *Molecular neurodegeneration,* **7**, pp. 8-1326-7-8.

ZHOU, X.W., LI, X., BJORKDAHL, C., SJOGREN, M.J., ALAFUZOFF, I., SOININEN, H., GRUNDKE-IQBAL, I., IQBAL, K., WINBLAD, B. and PEI, J.J., 2006. Assessments of the accumulation severities of amyloid beta-protein and hyperphosphorylated tau in the medial temporal cortex of control and Alzheimer's brains. *Neurobiology of disease,* **22**(3), pp. 657-668.

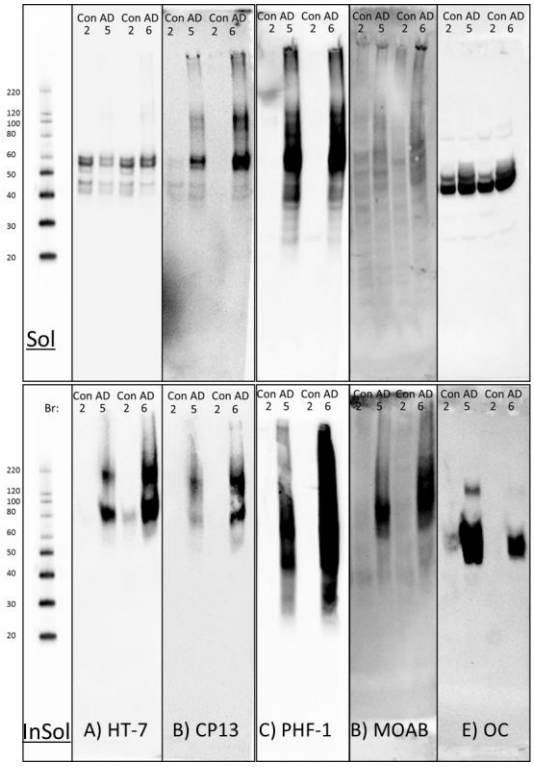

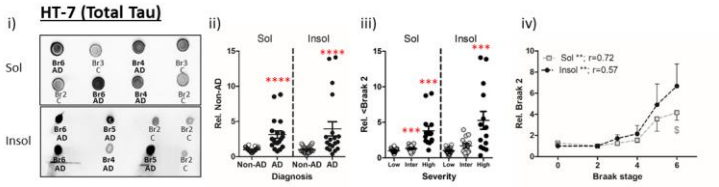

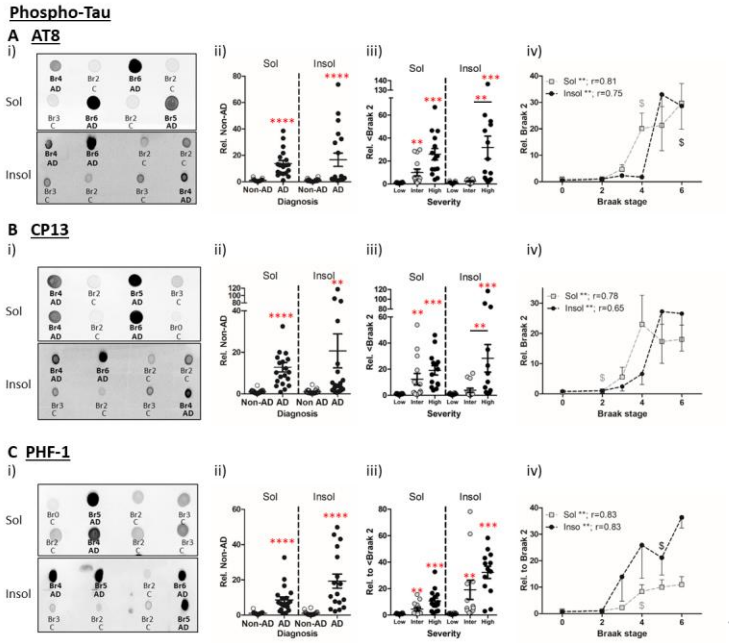

TOC1

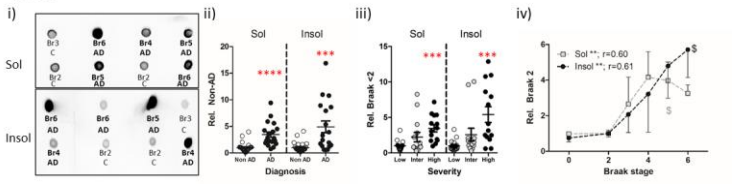

MOAB-2 Aβ

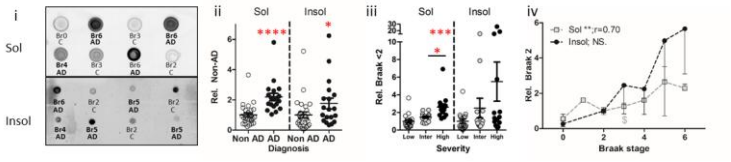

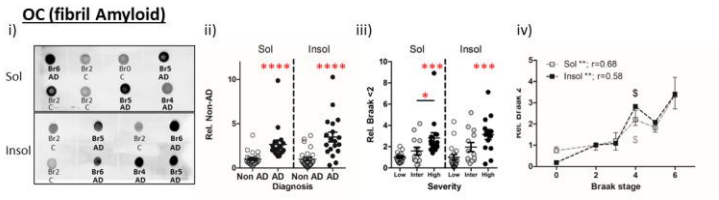

		MOAB-2		OC	
Marker	Solubility	Sol	Insol	Sol	Insol
HT7	Sol	0.5	NS	0.6	0.41
	Insol	NS	NS	0.6	NS
AT8	Sol	0.7	NS	0.7	0.44
	Insol	0.46	NS	NS	NS
CP13	Sol	0.63	NS	0.7	0.56
	Insol	0.54	NS	0.49	0.49
PHF1	Sol	0.67	NS	0.65	0.5
	Insol	0.5	NS	0.68	0.53
TOC1	Sol	0.52	NS	0.58	0.41
	Insol	0.4	NS	0.6	0.56

	Solubility	Braak	CERAD	MMSE	CDR	CDR memory	CDR SO
Total [HT-7]	S	**r=0.72 (NS)	**; r=0.76 (NS)	*; r=-0.55 (NS)	**; r=0.56 (NS)	**; r=0.59 (NS)	*; r=0.5 (NS)
	I	**r=0.57 (NS)	NS (NS)	NS (NS)	NS (NS)	NS (NS)	NS (NS)
Phospho [AT-8]	S	**; r=0.81 (**; r=0.71)	**; r=0.79 (NS)	**; r=-0.67 (NS)	**; r=0.69 (NS)	**; r=0.7 (NS)	**; r=0.6 (NS)
	I	**; r=0.75 (NS)	*; r=0.52 (NS)	*; r=-0.37 (NS)	*; r=0.36 (NS)	NS (NS)	NS (NS)
Phospho [CP13]	S	**; r=0.78 (**; r=0.65)	**; r=0.72 (NS)	**; r=-0.68 (NS)	**; r=0.69 (NS)	**; r=0.71 (*; r=0.56)	**; r=0.6 (NS)
	I	**; r=0.65 (NS)	**; r=0.66 (NS)	**; r=-0.67 (NS)	**; r=0.69 (NS)	**; r=0.63 (NS)	*; r=0.5 (NS)
Phospho [PHF-1]	S	**; r=0.83 (**=; r=0.66)	**; r=0.74 (NS)	**; r=-0.70 (NS)	**; r=0.68 (NS)	**; r=0.72 (NS)	*; r=0.5 (NS)
	I	**; r=0.83 (**; r=0.83)	**; r=0.80 (*;r=0.8)	**; r=0.69 (NS)	**; r=0.68 (NS)	**; r=0.67 (NS)	*; r=0.6 (NS)
Oligomeric [TOC1]	S	**; r=0.60 (NS)	**; r=0.62 (NS)	**; r=-0.59 (NS)	**; r=0.62 (NS)	**; r=0.62 (NS)	*; r=0.5 (NS)
	I	**; r=0.61 (NS)	**; r=0.65 (NS)	*; r=-0.54 (NS)	*; r=0.53 (NS)	*; r=0.5 (NS)	*r=0.49 (NS)
Aβ Total [MOAB-2]	S	**; r=0.70 (*; r=0.53)	**; r=0.69 (NS)	**; r=-0.69 (*; r=-0.58)	**; r=0.71 (**; r=0.70)	**; r=0.61 (*; r=0.53)	NS (NS)
	I	NS (NS)	NS (NS)	NS (NS)	*; r=0.49 (*; r=0.6)	NS (NS)	NS (NS)
Fibril amyloid [OC]	S	**; r=0.68 (NS)	**; r=0.67 (NS)	**; r=-0.58 (NS)	**; r=0.63 (NS)	**; r=0.62 (NS)	*; r=0.5 (NS)
	I	**; r=0.58 (NS)	**; r=0.60 (NS)	**; r=-0.54 (NS)	**; r=0.59 (*; r=0.6)	*; r=0.55 (NS)	NS (NS)

Braak stage	CERAD	N	Male (%)	Mean Age (years)	Age range (years)	Mean PMI (hrs)	PMI range (hrs)	Mean cortical pH	Cor r
0-3	C0-C2	27	44.4	86 ± 1.4	74-103	44.9 ± 5.2	11-110	6.3 ± 0.1	5
4-6	C2-C3	19	60	83.4 ± 1.2	71-90	46.6 ± 4.9	20-87	6.3 ± 0.1	6
hological severity									
0-2	C0-C1	18	66.7	85.3 ± 1.9	74-103	40.7 ± 6.2	11-92	6.3 ± 0.1	6
3-4	C0-C3	14	28.6	85.9 ± 1.5	77-95	51.5 ± 7	13.5-101	6.2 ± 0.2	5
5-6	C1-C3	14	71.4	83.6 ± 1.5	71-90	46 ± 5.7	20-78	6.4 ± 0.1	6
e									
0	C0	3	100	76.7 ± 1.3	74-78	30 ± 13.5	11-56	6.1 ± 0.1	6
1	-	0	-	-	-	-	-	-	
2	C0-C1	15	40	87 ± 2	74-103	42.8 ± 7	12-92	6.3 ± 0.1	6
3	C0-C2	9	33.3	87.6 ± 1.7	78-95	53.4 ± 9.5	13.5-101	6.2 ± 0.3	5
4	C2-C3	5	40	82.8 ± 2.2	77-88	48.2 ± 10.6	26-87	6.2 ± 0.2	6
5	C1-C3	6	83.3	83.8 ± 1.2	82-88	50.5 ± 10.1	22-78	6.3 ± 0.1	6
6	C3	8	50	83.5 ± 2.4	71-90	42.6 ± 6.9	20-69	6.5 ± 0.1	6

Antibody	Epitope	Specificity	Dilution	Supplier
HT7	aa 159-163 of tau	Pan-tau	1:5000	Autogen Bioclear
AT8	pSer199/202 +pThr205	Phospho-tau	1:50	Autogen Bioclear
CP13	pSer202	Phospho-Tau	1:250	P.Davies Lab
PHF-1	pSer396/404	Phospho-Tau	1:1000	P.Davies Lab
TOC1	epitope preferentially exposed when oligomerised; aa 209-244	Oligomeric Tau	1:5000	N. Kanaan / L. Binder Lab
6E10	aa 3-8 of Aβ	APP and metabolites (Aβ)	1:1000	Biolegend
MOAB-2	aa 1-4 of Aβ	Aβ only	1:1000	Biosensis
OC	sequence independent, conformational epitope	Amyloid fibrils	1:1000	Millipore

Highlights

- Two distinct phospho-dependent profiles of insoluble tau deposition are apparent.
- Soluble tau and Aβ better correlate with AD progression than insoluble measures.
- Soluble tau and Aβ better correlate with cognitive decline than insoluble measures.
- Soluble Aβ correlate with cognitive decline following end stage case exclusion.
- Insoluble fibril amyloid better correlates with AD progression than total Aβ.